UV and Infrared absorption spectra and 248 nm photolysis of maleic anhydride ($C_4H_2O_3$)

Paul Marshall,[1,2,#] Vassileios C. Papadimitriou,[1,2,$] , Dimitrios K. Papanastasiou,[1,2]
James M. Roberts,[2] and James B. Burkholder[2 *]

[1] Earth System Research Laboratory, Chemical Sciences Division, National Oceanic and Atmospheric Administration, 325 Broadway, Boulder, CO, USA 80305-3328
[2] Cooperative Institute for Research in Environmental Sciences, University of Colorado, Boulder, CO, USA 80309

Permanent address: Department of Chemistry, University of North Texas, 1155 Union Circle #305070, Denton, Texas 76203, USA
[$] Permanent Address: Laboratory of Photochemistry and Chemical Kinetics, Department of Chemistry, University of Crete, Heraklion, Crete, Greece.

Journal of Photochemistry and Photobiology A: Chemistry

Running Title: Maleic Anhydride Spectroscopy

* Corresponding author:
J.B. Burkholder
email: james.b.burkholder@noaa.gov
Ph: 303-497-3252
ORCID: 0000-0001-9532-6246

Abstract

Maleic anhydride ($C_2H_2(CO)_2O$, Furan-2,5-dione) is emitted into or formed in the atmosphere during bio-mass burning events as well as being a photochemical degradation product of some aromatic volatile organic compounds. The photochemical fate of maleic anhydride, however, is presently not well enough characterized to enable modeling of its impact on the environment and human health. Maleic anhydride is a strong UV absorbing molecule with a continuous spectrum that extends well into the long-wavelength atmospheric actinic region, >295 nm. In this study, the room temperature UV and infrared absorption spectra of maleic anhydride were measured and quantified using several complementary calibration methods. In addition, photolysis quantum yields and stable end-product yields were measured following its 248 nm pulsed laser photolysis. Photoproducts were measured at room temperature using Fourier transform infrared spectroscopy detection under slow flow conditions at total pressures in the range 100–600 Torr (Syn Air). The maleic anhydride photolysis quantum yield was determined to be 0.85 ± 0.20, independent of pressure, with CO, CO_2, and acetylene (C_2H_2) photo-products formed with a 1:1:1 stoichiometric ratio and a yield of 1 ± 0.15, independent of total pressure.

1. Introduction

Biomass burning is a significant atmospheric source of aromatic and heterocyclic compounds from primary emission and secondary photochemical processing [1, 2]. The atmospheric photochemical degradation of these compounds impacts ozone production, aerosol formation and visibility, and human health on local, regional, and global scales. A thorough understanding of the atmospheric loss processes and atmospheric photochemical degradation mechanisms of these compounds is, therefore, a key element in the development of reliable air quality modeling.

Maleic anhydride (Furan-2,5-dione, $C_4H_2O_3$, MA), shown in **Fig. 1**, is a heterocyclic furan-type compound recently identified as a product in bio-mass burning [1, 3, 4]. Maleic anhydride is thought to be a second generation bio-mass burning product formed in the degradation of furfural (Furan-2-carbaldehyde, $C_5H_4O_2$) [5]. In addition, maleic anhydride is formed in the oxidation of simple aromatic hydrocarbons,[6, 7] through intermediates that have alkene-dial structures [8, 9]. There are currently limited reactivity and spectroscopic data available for maleic anhydride. Bierbach et al. [8] performed a relative rate kinetic study of the OH radical reaction with-maleic anhydride and report a room temperature rate coefficient of 1.45 $\times$ 10^{-12} cm^3 $molecule^{-1}$ s^{-1}. Reaction with the OH radical therefore leads to a relatively short lifetime of maleic anhydride in the troposphere, ~8 days. To the best of our knowledge, the products of the OH radical reaction with maleic anhydride have not yet been identified. Back and Parsons [10] reported a UV absorption spectrum of maleic anhydride between 250–400 nm at an elevated temperature of 420 K. Although measured at an elevated temperature, it is clear that maleic anhydride absorbs strongly in the long-wavelength solar actinic region, λ >295 nm. Back and Parsons [10] also reported the formation of CO, CO_2, and C_2H_2 as stable end-products in the broadband, 220 to 350 nm, photolysis of maleic anhydride:

$$C_4H_2O_3\ (MA) + h\nu \rightarrow CO + CO_2 + C_2H_2 \qquad (1)$$

where the photolysis occurs via a concerted or stepwise mechanism, i.e., the dynamics of maleic anhydride photolysis have not been characterized to date. Absolute quantum yields were not determined in the Back and Parsons [10] study. Bierbach et al. [8] also observed these same photolysis products following 254 nm fluorescent lamp photolysis, but the quantum and product yields were not quantified.

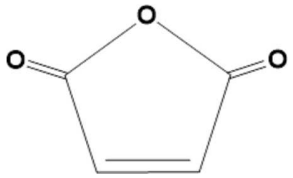

Maleic Anhydride

Fig. 1. Maleic Anhydride (Furan-2,5-dione)

The focus of the present study was on the determination of quantitative UV and infrared absorption spectra and the 248 nm photochemistry of maleic anhydride. Maleic anhydride is a low-volatility compound and an emphasis in this work was placed on establishing reliably calibrated spectroscopic data for use in future laboratory kinetic studies and for the calibration of instruments used to measure maleic anhydride in the environment. Maleic anhydride quantum yields following 248 nm pulsed laser photolysis and stable end-product yields were studied to provide insights into its photolysis mechanism and atmospheric photochemistry.

2. Experimental Details

In this study, UV and infrared absorption spectra of maleic anhydride and photolysis quantum yields following 248 nm pulsed laser photolysis were measured. The UV and infrared absorption cross sections determined in this work were used in the analysis of the 248 nm photolysis experiments. The apparatus and methods used in this study are described separately below.

2.1 UV Absorption Spectrum

Gas-phase UV absorption spectra, $\sigma(\lambda)$, were determined by applying Beer's law:

$$A(\lambda) = \sigma(\lambda) \times L \times [\text{Maleic Anhydride}] \quad \text{(I)}$$

where $A(\lambda)$ is the measured absorption at wavelength λ, $\sigma(\lambda)$ is the absorption cross section of maleic anhydride , L is the absorption pathlength, and [maleic anhydride] is the maleic anhydride concentration.

Maleic anhydride absorption cross sections were measured over the wavelength range 200–360 nm using a charge couple device (CCD) detector equipped spectrometer and at 213.9 nm (Zn lamp) and 228.8 nm (Cd lamp) using atomic lamps. Atomic line absorption

measurements were made using Pen-ray lamp light sources, Pyrex absorption cells with quartz windows, and photodiode detectors with bandpass filters for the atomic wavelengths. Absorption cells with pathlengths of 10, 25, and 100 cm were used over the course of the measurements. Broadband spectra were measured using a 30 W D_2 lamp, 90.4 cm single pass absorption cell, and a 0.5 m spectrometer with a 512 × 2048 cooled CCD detector. All measurements were performed at 296 K.

The maleic anhydride concentration was quantified using two independent calibration methods: (1) absolute pressure measurements of dilute maleic anhydride mixtures prepared manometrically off-line, and (2) maleic anhydride sample combustion and total conversion of the carbon in maleic anhydride to CO_2 [11]. The measurement of maleic anhydride by combustion was accomplished using a platinum catalyst as described by Stockwell et al. [12], followed by measurement of the resulting CO_2 by non-dispersive infrared detection (NDIR, LI-COR 6251) [11]. A gas stream of maleic anhydride in zero air was produced by passing zero air over the solid held at 65 °C. The maleic anhydride mixing ratios ranged from 102 to 586 ppmv at room pressure (630 ± 1.2 Torr) by variation of a gas flow dilution. The NDIR instrument was operated in the absolute mode, i.e., with a CO_2 scrubbed reference cell, with 10 s averaging. The measurement channel was zeroed using a magnesium perchlorate/sodium carbonate scrubber. The NDIR instrument was calibrated using a set of carbon standards as shown in the supplementary material (**Fig. S1**). Calibration checks, using the 399 ± 4 ppmv CO_2 and 200 ± 4 ppmv CO standards, were performed during the maleic anhydride experiments. The uncertainties in the standards when combined with the uncertainties in the zero (±0.27 ppmv), the measurement (±0.27 ppmv), and the fact that the highest maleic anhydride measurements were slightly above the calibrated range, yields an estimated overall uncertainty of ~4% for the maleic anhydride concentration measurement.

Prior to the gas flow entering the combustion apparatus, the maleic anhydride gas mixture passed through a 10.2 cm long 213.9 nm (Zn lamp) absorption cell. The maleic anhydride concentration determined by combustion was used in eq. I to determine the 213.9 nm absorption cross section, σ(213.9 nm). This method provided a direct determination of σ(213.9 nm) relative to the CO_2 produced. The accuracy of the UV absorbance measurement was ~2% and the absolute uncertainty in σ(213.9 nm) is estimated to be ~5%.

The UV absorption spectrum of maleic anhydride between 200 and 360 nm spans 4 orders of magnitude in its absorption cross section. To optimize the spectrum determination in the broadband CCD spectrometer measurements over this range, the measurements and maleic anhydride concentration were optimized for the <230 nm and >220 nm regions and combined using the overlapping region (220 and 230 nm) to obtain the final spectrum. Measurements were made by flowing a dilute maleic anhydride mixture (0.01%) through two absorption cells mounted in series, a 90.4 cm long cell for the CCD broadband absorption measurement and a 105.5 cm long cell for Zn and Cd atomic line absorption measurements. This combination of absorption measurements enabled direct comparison with the combustion results described above.

2.2 Infrared Absorption Spectrum

The maleic anhydride infrared absorption spectrum was quantified using absolute pressure measurements as well as measurements relative to the Zn atomic line cross section determined in the combustion experiments described above. Spectra were measured at 296 K using Fourier transform infrared (FTIR) spectroscopy between 500 and 4000 cm^{-1} at 0.5 cm^{-1} resolution. The FTIR was coupled to a multi-pass absorption cell (KBr windows) with a 485 cm optical pathlength. The detector was a liquid nitrogen cooled HgCdTe (MCT) semi-conductor.

In the relative cross section determination, a slow flow of a maleic anhydride gas sample passed through a 25 cm long 213.9 nm absorption cell before entering the FTIR absorption cell. Another 213.9 nm absorption cell was placed at the exit of the FTIR to confirm no loss of maleic anhydride when flowing through the system. In the absolute method, maleic anhydride samples were taken from dilute mixtures in a He bath gas prepared manometrically off-line. Spectra were measured under slow flow conditions. The maleic anhydride concentration was calculated using the measured absolute pressure, the mixing ratio of the dilute sample, and the ideal gas law. The range of concentration used in the absorption measurements was $(1.37–3.29) \times 10^{14}$ molecule cm^{-3}. Background spectra were recorded with the absorption cell filled with the He bath gas. A linear least-squares fit of the infrared data integrated over the range 1700–2000 cm^{-1} to eq. (I) was used to obtain the final spectrum.

2.3 Quantum and Photolysis Product Yields

Maleic anhydride photolysis quantum yields, $\Phi(\lambda)$, following 248 nm pulsed laser (KrF excimer laser) photolysis were determined by measuring the loss of maleic anhydride relative to the loss of a reference compound, Halon-2402 ($CBrF_2CBrF_2$). Quantum yields were measured by following the loss of maleic anhydride and Halon-2402, by UV and infrared absorption, in separate experiments under identical pressure and gas flow conditions. Maleic anhydride flowed through a 100 cm long (1" o.d.) photolysis cell, then through a 25 cm long 213.9 nm absorption cell, and then through the FTIR multi-pass absorption cell. Maleic anhydride was exposed to multiple photolysis laser pulses while in the reactor to achieve measurable changes in its concentration. The extent of exposure to the photolysis laser was varied by adjusting the residence time in the photolysis cell and the repetition rate of the photolysis laser between 10 and 40 Hz with 10–18 mJ cm^{-2} $pulse^{-1}$.

The fraction of maleic anhydride remaining after photolysis per laser pulse is given by:

$$\frac{[MA]}{[MA]_0} = (1 - \Phi_{MA}\sigma_{MA}F) \quad \text{(II)}$$

where Φ_{MA} is the maleic anhydride quantum yield and F is the photolysis laser fluence (photons cm^{-2} $pulse^{-1}$). For a small fractional loss per pulse, after n laser pulses (i.e., laser frequency × time) the remaining maleic anhydride is approximated as:

$$\frac{[MA]_n}{[MA]_0} = (1 - \Phi_{MA}\sigma_{MA}F)^n \quad \text{(III)}$$

A plot of $\ln([MA]_0/[MA]_n)$ vs n yields $\Phi_{MA}\sigma_{MA}F$ as the slope, m_{MA}. The same expression can be written for the Halon reference compound. For a constant photolysis laser fluence, the ratio of MA and Halon slopes yields the maleic anhydride quantum yield via:

$$\Phi_{MA}(\lambda) = \Phi_{Halon}(\lambda) \times \frac{m_{MA}}{m_{Halon}} \times \frac{\sigma_{Halon}(\lambda)}{\sigma_{MA}(\lambda)} \quad \text{(IV)}$$

where $\Phi_{Halon}(248.3\ nm) = 1$, $\sigma_{Halon}(248.3\ nm) = 5.25 \times 10^{-20}$ cm^2 $molecule^{-1}$-[13] $\sigma_{MA}(248.3\ nm) = 8.02 \times 10^{-20}$ cm^2 $molecule^{-1}$ (this work). (The effective KrF excimer wavelength is 248.3 nm).

Product yields, Υ, were measured simultaneously during the quantum yield experiments by monitoring the formation of stable end-products by infrared absorption relative to the loss of maleic anhydride:

193 $$\Upsilon_{Product} = \frac{[Product]}{\Delta[\text{maleic anhydride}]} \quad \text{(V)}$$

194 *2.4 Materials*. Maleic anhydride ($C_2H_2(CO)_2O$, Furan-2,5-dione, CAS RN: 108-31-6), a
195 low-vapor pressure (~0.2 Torr) solid at room temperature, was obtained commercially with a
196 stated purity of >99%. The maleic anhydride sample was stored in a glass vacuum reservoir and
197 thoroughly degassed prior to use. Dilute mixtures of maleic anhydride in a He bath gas, 0.0104
198 and 0.0145% with a total pressure of ~800 Torr, were prepared manometrically in a 12 L Pyrex
199 bulb with a mixing ratio estimated uncertainty of ~2%. The maleic anhydride bulb mixtures
200 were stable over the duration of the study as confirmed by repeated infrared absorption
201 measurements. N_2 (UHP, 99.999%), He (UHP, 99.999%), and zero Air (UHP, 99.999%) were
202 used as supplied. $CBrF_2CBrF_2$ (Halon-2402, 99%) was used as supplied. A Halon-2402 mixture
203 in a He bath gas, ~5%, was prepared manometrically and used in the photolysis experiments.
204 Pressures were measured using calibrated 10, 100, and 1000 Torr capacitance manometers.
205 Uncertainties given throughout the paper are 2σ unless noted otherwise.

206 **3. Results and Discussion**

207 *3.1 UV Absorption Spectrum*

208 The maleic anhydride UV absorption spectrum was quantified at the 213.9 nm (Zn) and
209 228.8 nm (Cd) atomic lines. The spectrum obtained over the wavelength range 200 to 360 nm
210 was scaled to the 228.8 nm cross section value. The atomic line cross section values and
211 broadband spectrum is shown in **Fig. 2**. **Table S1** provides cross section data between 200 and
212 360 nm at 0.5 nm intervals. Over the 200–360 nm wavelength range the maleic anhydride
213 spectrum spans cross sections of nearly four orders of magnitude with two electronic transitions
214 with peaks below 200 nm and at ~310 nm clearly apparent. The spectrum shows diffuse band
215 structure at wavelengths in the range 200–218 nm and 250–360 nm. The electronic transitions
216 were assigned in the study of Back and Parsons [10] to a $\pi \leftarrow \pi^*$ transition that extends from our
217 short wavelength limit out to ~260 nm and overlapping weaker $\pi \leftarrow n_+$ and $\pi \leftarrow n_+$ transitions at
218 longer wavelengths.

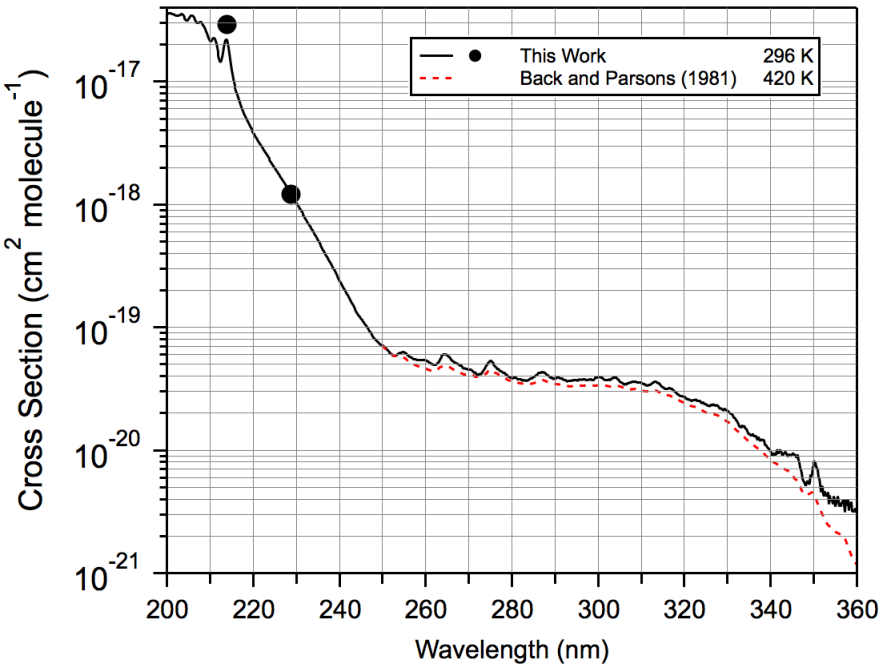

Fig. 2. UV absorption spectrum of maleic anhydride ($C_2H_2(CO)_2O$) at 296 K measured in this work at 213.9 and 228.8 nm (solid circles) using atomic lamps and broadband (200–360 nm) (solid line) measured using a CCD spectrometer. Absorption cross sections are given in **Table S1**. The spectrum reported by Back and Parsons [10] at 420 K (dashed line) is included for comparison.

Fig. 3 and 4 show the results from the quantitative cross section determinations at 213.9 and 228.8 nm, respectively. **Fig. 3** shows the results obtained at 213.9 nm using the prepared mixture of maleic anhydride diluted in a He bath gas and using the combustion method. The cross sections obtained from the two datasets agree to within 2%, while the absolute method shows a slight non-zero intercept. The cross section at 213.9 was determined from the combustion experiments to be $(3.06 \pm 0.06) \times 10^{-17}$ cm^2 molecule^{-1}. As shown in **Fig. 2**, there is a difference between the 213.9 nm cross section obtained using the Zn atomic lamp, which is greater, and the CCD spectrometer measurement. We attribute the difference in cross section to the difference in measurement resolution in the short-wavelength structured region of the maleic anhydride spectrum. That is, the CCD measurement (~1 nm resolution) does not resolve the structure of the spectrum adequately. In part to confirm this hypothesis, cross section measurements were also performed at the Cd atomic line. **Fig. 4** shows the absolute cross section measurements at the 228.8 nm Cd line that yields a cross section of $(1.21 \pm 0.02) \times 10^{-18}$ cm^2 molecule^{-1}. A limited number of CCD absolute cross section measurements yielded cross

sections in excellent agreement with the Cd result, agreement to within 2%. The final broadband CCD spectrum shown in **Fig. 2** and listed in **Table S1** was scaled to the Cd line cross section determination. The agreement between the atomic lamp and CCD measurements is much better at 228.8 nm (Cd lamp) than at 213.9 nm, because it falls in a wavelength region of the maleic anhydride spectrum that does not exhibit structure.

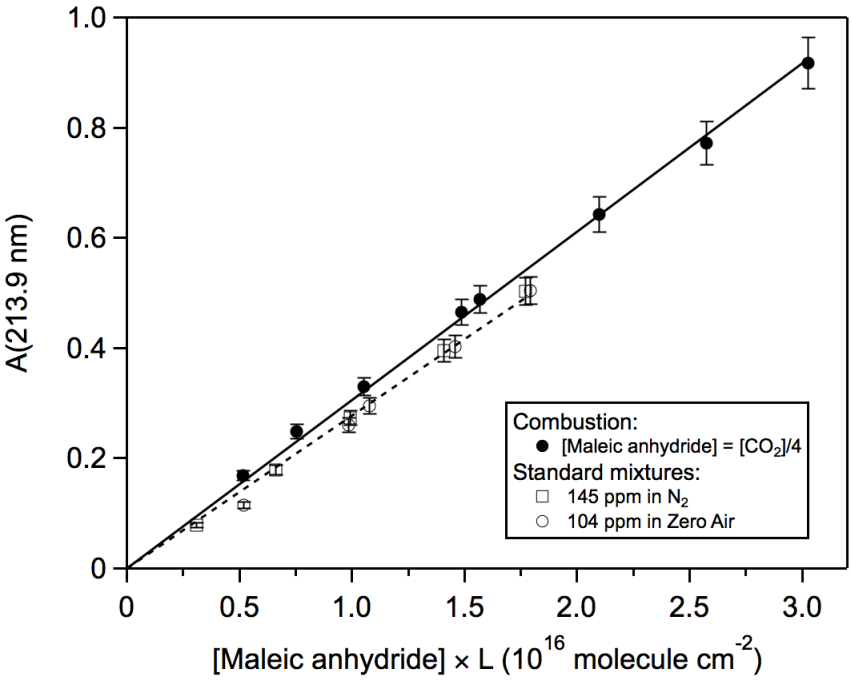

Fig. 3. Maleic anhydride absorption cross section data at 213.9 nm (Zn line) obtained using two independent methods. The combustion data measured the 213.9 nm absorption signal with an absorption pathlength (L) of 10.2 cm. The absolute measurement approach used an absorption cell with L = 100.5 cm. Data point error bars are ±5%. The lines are linear least-squares fits of the data.

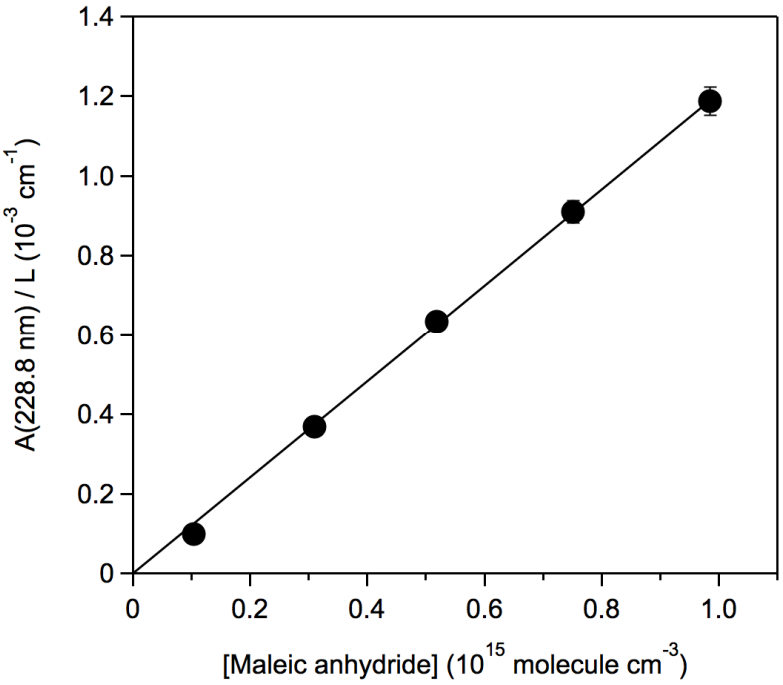

Fig. 4. Maleic anhydride absorption cross section data at 228.8 nm (Cd line) obtained using an atomic lamp (L = 100.5 cm). The line is a linear least-squares fit of the data forced through the origin.

The absolute uncertainty in the maleic anhydride UV cross sections was estimated from the precision of the atomic lamp measurements, the agreement between the calibration methods, and the accuracy of the CCD measurement. The calibration methods used in the 213.9 nm cross section determination agreed very well with an estimated uncertainty of ~2%. The precision of the atomic lamp measurements was high with an estimated uncertainty of <1%. The estimated uncertainty in the CCD measured spectrum is wavelength dependent with the largest uncertainty associated with the weakest recorded absorption signals. The absolute uncertainty in the 200 to 280 nm range is estimated to be ~5%, 280 to 340 nm is ~10%, with an increasing uncertainty toward longer wavelengths up to ~100% at 360 nm.

Back and Parsons [10] reported a maleic anhydride spectrum between 250 and 360 nm that was recorded at 420 K. Their spectrum compares favorably with the present room temperature spectrum, although our spectrum in this region is ~20% greater, see **Fig. 2** for a comparison of the spectra.

3.2 Infrared Absorption Spectrum

The infrared absorption spectrum of maleic anhydride was determined relative to the 213.9 nm cross section and by complementary absolute measurements. The Beer's law data obtained using the Zn method is summarized in **Fig. S2**. The agreement between the two methods is good, better than 5%. The recommended infrared absorption spectrum, obtained relative to the 213.9 nm absorption cross section, is shown in **Fig. 5** and a digitized spectrum is given in the SI. The integrated band strength in the 1700–2000 cm^{-1} region was determined to be 9.00×10^{-17} cm^2 $molecule^{-1}$ cm^{-1}. Note that the reported spectrum shows some artifacts in the regions around the strong under-resolved Q-branches.

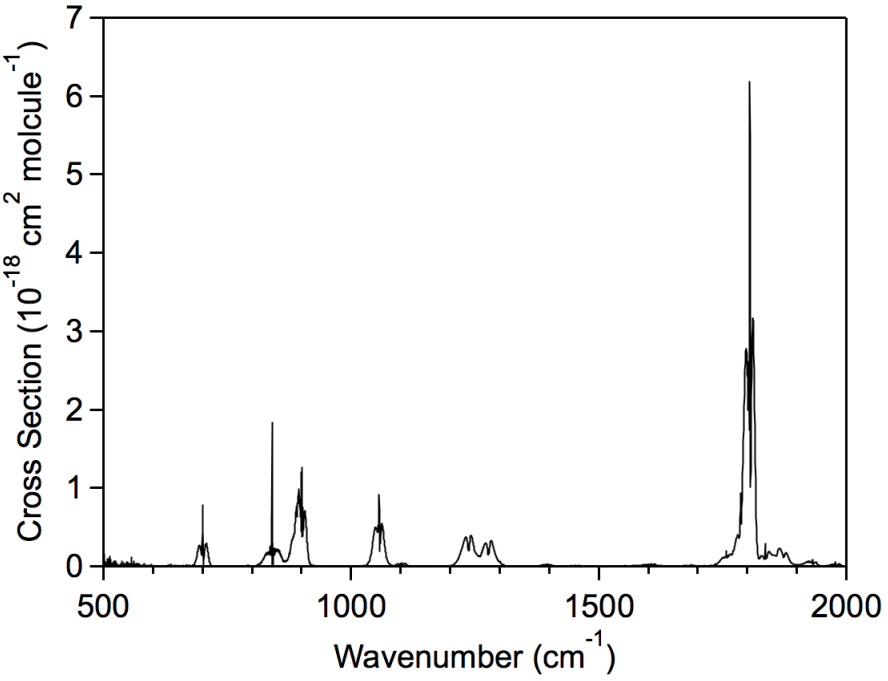

Fig. 5. Infrared absorption spectrum of maleic anhydride ($C_2H_2(CO)_2O$) at 296 K measured in this work. A digitized spectrum is given in the SI.

Assignments of the major bands in the infrared spectrum of maleic anhydride were assisted by anharmonic frequency calculations made with density functional theory. The 6-311+G(3df,2p) basis set was combined with the B3LYP and M06-2X functionals. These calculations allow for overtones and combination bands and the results are listed in **Table 1**.

Table 1

Observed band centers in the infrared spectrum of maleic anhydride and normal mode assignments based on comparison with anharmonic frequency calculations made with density functional theory

Band center (cm^{-1})	Assignment	Symmetry and description
702	ν_{20}	B2 ring deformation
842	ν_{12}	B1 C-H out-of-plane bends
900	ν_{19}	B2 antisymmetric C-O stretches
1058	ν_{18}	B2 antisymmetric C-C stretches
1102	ν_5	A1 symmetric C-C-H bends
1236	ν_4	A1 symmetric C-O stretches
1277	2 ν_7 and/or $\nu_6 + \nu_8$	ν_6 is A1 symmetric C-C stretch, ν_7 is A1 C-O-C bend, ν_8 is A1 symmetric O=C-O bends
1394	ν_{17}	B2 non-symmetrical C-C-H bends
1608	ν_3	A1 C=C stretch
1805	ν_{16}	B2 asymmetric C=O stretches
1838	$\nu_4 + \nu_{21}$	ν_{21} is B2 antisymmetric O=C-O bends
1874	$\nu_6 + \nu_{18}$	ν_6 is A1 ring expansion
1935	ν_2	A1 symmetric C=O stretch
1980	$\nu_4 + \nu_{20}$	
3651	$\nu_2 + \nu_{16}$	

3.3 248 nm Photolysis

The photolysis quantum yield of maleic anhydride and product yields were measured at 296 K at total pressures of 101, 204, 406, and 600 Torr (Zero Air) under slow flow conditions. The conditions of the experiments and obtained quantum yields are given in **Table 2**. Representative quantum yield data obtained at 600 Torr total pressure is shown in **Fig. 6**. The loss of maleic anhydride and the reference compound, Halon-2402, was linear to within ~2%. The quantum yield was found to be independent of pressure over this pressure range with an average value of 0.85 ± 0.15. The estimated overall uncertainty, including estimated systematic errors, of 20% does not exclude a unit quantum yield.

Table 2

Summary of maleic anhydride ($C_2H_2(CO)_2O$, MA) 248 nm photolysis quantum yield measurements at 296 K from this work

Total Pressure (Torr, Zero Air)	$[Halon\text{-}2402]_0$ (10^{15} molecule cm^{-3})	$[Maleic\ anhydride]_0$ (10^{14} molecule cm^{-3})	m_{Halon} (10^{-3})	m_{MA} (10^{-3})	m_{MA}/m_{Halon}	Quantum Yield [a]

609	6.0	2.13	1.89 ± 0.02	2.57 ± 0.04	1.360	0.846 ± 0.033
406	2.6	2.16	1.66 ± 0.04	2.17 ± 0.05	1.307	0.815 ± 0.057
204	3.2	2.14	1.65 ± 0.03	2.26 ± 0.04	1.370	0.854 ± 0.043
101	3.4	2.15	1.76 ± 0.02	2.43 ± 0.004	1.381	0.860 ± 0.020

[a] See Eq. IV; Linear flow velocity was 27 cm s^{-1}; Quoted uncertainties are 2σ fit precision values.

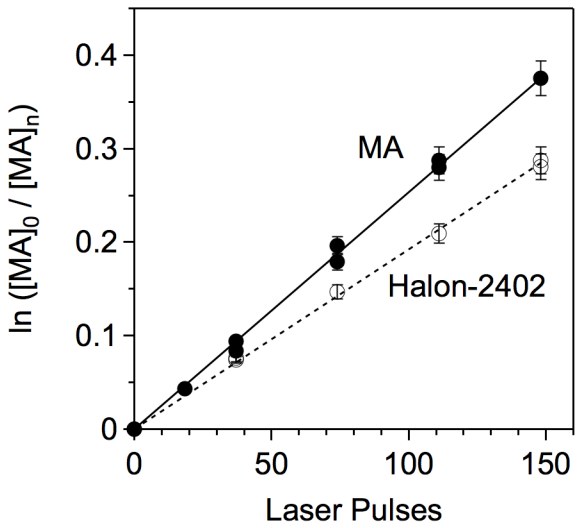

Fig. 6. Maleic anhydride ($C_2H_2(CO)_2O$, MA) (solid circles) and Halon-2402 ($CBrF_2CBrF_2$) reference gas (open circles) 248 nm photolysis quantum yield data obtained at 296 K in 600 Torr (Zero Air) bath gas. Data error bars are ±5%. The lines are linear least-squares fits to the data. A summary of the quantum yields obtained in this work is given in **Table 2**.

CO, CO_2, and C_2H_2 (acetylene) were the only photolysis products observed using infrared absorption detection. Representative product yield data is shown in **Fig. 7**. The CO, CO_2, and C_2H_2 products showed a 1:1:1 stoichiometry with a unit yield to within the precision of the measurements. Note that the error bars shown in **Fig. 7** are primarily due to the uncertainty in the spectral subtraction of standard reference spectra and the fact that our low-resolution absorption measurements do not fully resolve rotational structure. The observation of CO, CO_2, and C_2H_2 as major photolysis products is consistent with the qualitative observations in the previous studies of Back and Parsons [10] and Bierbach et al. [8]. Our experiments are not sensitive to the mechanism of maleic anhydride photolysis, i.e., the formation of the observed products could be a concerted or step-wise mechanism. However, in either case, 248 nm photolysis ultimately leads to the rupture of two carbon-carbon bonds and one carbon-oxygen

bond in the ring. Maleic anhydride is not aromatic and the carbonyl groups are expected to be the active chromophores that drive the photochemistry.

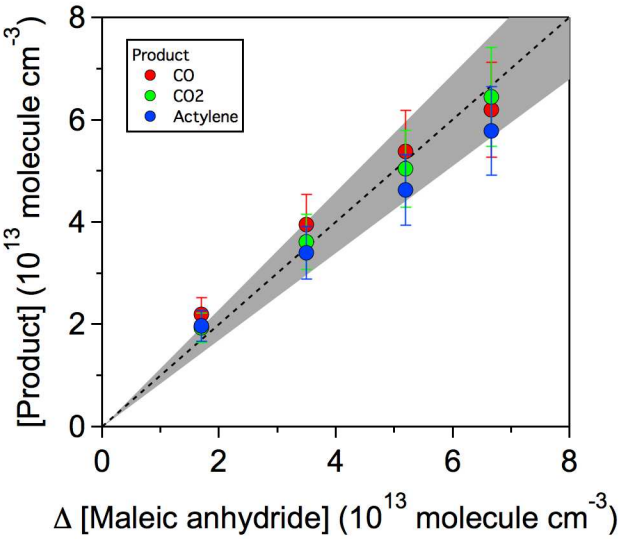

Fig. 7. CO, CO_2, and acetylene product yield data in the 248 nm photolysis of maleic anhydride in 600 Torr (Zero Air) bath gas (see **Figure 4**). The data point error bars are ±15%. The dashed line corresponds to a unit molar yield. The gray shaded region represents ±15% around the 1:1 line. Data obtained at 101, 204, and 406 Torr total pressure yield similar quality data.

At 298 K the reaction enthalpy for the decomposition of maleic anhydride to CO, CO_2, and C_2H_2 products is 125 kJ mol^{-1} [14, 15], and the activation energy for its thermal reaction has been measured to be 254 kJ mol^{-1} [10]. The corresponding wavelength threshold for photolysis to these products is 955 nm, which is well below the energy input by the 248 nm excitation used in the present photolysis experiments. We have made a preliminary exploration of the excited states of maleic acid computationally, using time-dependent density functional theory as implemented in Gaussian16 [16]. B3LYP/6-311+G(3df,2p) excitations were evaluated at the B3LYP/6-311G(d,p) $^1A_1$ ground-state geometry. Predicted wavelengths for vertical transitions and the associated oscillator strengths are listed in **Table 3**. There are several low-lying states that are energetically accessible by photons in the solar actinic region of the spectrum, but their transitions from the ground state are spin and/or symmetry forbidden in this C_{2v} molecule. Coupling to vibrations presumably accounts for the weak absorption observed in the actinic

wavelength region (see **Fig. 1**). The measured rise in absorption cross section below 250 nm correlates with allowed transitions to two $^1B_2$ excited states.

Alternative to direct photodissociation, Back and Parsons [10] have proposed that maleic anhydride dissociation may occur via rapid internal conversion (IC) to the ground electronic state with subsequent dissociation along pathways similar to thermal decomposition, but with greater internal energy. Our experiments are not able to differentiate between direct photodissociation and such an IC mechanism. Our observed independence of the quantum yield on pressure (100 to 600 Torr) does, however, imply that excited energy levels with lifetimes longer than ~1 ns are not involved in the dissociation process.

Table 3

Excited electronic states of maleic anhydride calculated relative to the $^1A_1$ ground state using time-dependent density functional theory at the B3LYP/6-311+G(3df,2p) level of theory

State symmetry	Vertical transition wavelength (nm)	Oscillator strength
$^3B_1$	381	0
$^3B_2$	373	0
$^1B_1$	337	0
$^3A_2$	313	0
$^1A_2$	282	0
$^3B_2$	281	0
$^1B_2$	230	0.007
$^3A_1$	210	0
$^1B_2$	209	0.318
$^3A_2$	188	0

Photolysis experiments were also attempted using 213.9 Zn lamp photolysis. Although the maleic anhydride cross section is high at this wavelength and photodissociation of maleic anhydride was observed, the Zn lamp intensity was not sufficient to obtain quantitative quantum yield data. CO, CO_2, and acetylene were observed as photolysis products in these photolysis experiments.

4. Summary

This study provided accurately calibrated UV and infrared spectra for maleic anhydride. Maleic anhydride absorbs strongly in the UV region and its absorption spectrum extends well into the atmospheric photolysis actinic region, λ >295 nm, with significant cross sections. The

photolysis of maleic anhydride at 248 nm was shown to proceed with a near unit quantum yield and lead to unity molar yields of CO, CO_2, and C_2H_2. In addition to studies of other possible maleic anhydride atmospheric loss processes, photolysis quantum yield and product studies at wavelengths more relevant to atmospheric photolysis are needed for an accurate evaluation of its impact on the environment.

Acknowledgements

This work was supported in part by NOAA Climate Program Office Atmospheric Chemistry, Carbon Cycle, and Climate Program and NASA's Atmospheric Composition Program.

Supplementary Material

* Maleic anhydride infrared absorption spectrum in JCAMP format
* Table S1: Maleic anhydride UV cross section data
* Figure S1: CO_2 instrument calibration data
* Figure S2: Beer's law data for the maleic anhydride infrared band strength

References

[1] A.R. Koss, K. Sekimoto, J.B. Gilman, V. Selimovic, M.M. Coggon, K.J. Zarzana, B. Yuan, B.M. Lerner, S.S. Brown, J.-L. Jimenez, J. Krechmer, J.M. Roberts, C. Warneke, R.J. Yokelson, J. de Gouw, Non-methane organic gas emissions from biomass burning: identification, quantification, and emission factors from PTR-ToF during the FIREX 2016 laboratory experiment, Atmos. Chem. Phys., 18 (2018) 3299-3319.

[2] J.B. Gilman, B.M. Lerner, W.C. Kuster, P.D. Goldan, C. Warneke, P.R. Veres, J.M. Roberts, J.A. de Gouw, I.R. Burling, R.J. Yokelson, Biomass burning emissions and potential air quality impacts of volatile organic compounds and other trace gases from fuels common in the US, Atmos. Chem. Phys., 15 (2015) 13915-13938.

[3] A. Hartikainen, P. Yli-Pirilä, P. Tiitta, A. Leskinen, M. Kortelainen, J. Orasche, J. Schnelle-Kreis, K.E. Lehtinen, R. Zimmermann, J. Jokiniemi, O. Sippula, Volatile organic compounds from logwood combustion: Emissions and transformation under dark and photochemical aging conditions in a smog chamber, Environ. Sci. Technol., 52 (2018) 4979-4988.

[4] M.M. Coggon, C. Lim, A.R. Koss, K. Sekimoto, B. Yuan, C. Cappa, J. Kroll, V. Selimovic, K. Zarzana, S. Brown, J.M. Roberts, M. Müller, R. Yokelson, A. Wisthaler, J. Krechmer, J. Jimenez, J. de Gouw, C. Warneke, OH-chemistry of volatile organic compounds emitted from laboratory and ambient biomass burning smoke: Influence of furans and oxygenated aromatics on ozone and secondary VOC formation, in preparation, (2019).

[5] X. Zhao, L. Wang, Atmospheric oxidation mechanism of furfural initiated by hydroxyl radicals, J. Phys. Chem. A, 121 (2017) 3247-3253.

[6] H. Bandow, N. Washida, Ring-cleavage reactions of aromatic hydrocarbons stidied by FT-IR spectroscopy. II. Photooxidation of *o*-, *m*-, and *p*-xylenes in the NO_x-air system, Chem. Soc. Japan, 58 (1985) 2541-2548.

[7] H. Bandow, N. Washida, H. Akimoto, Ring-cleavage reactions of aromatic hydrocarbons stidied by FT-IR spectroscopy. I. Photooxidation of toluene and benzene in the NO_x-air system, Chem. Soc. Japan, 58 (1985) 2531-2540.

[8] A. Bierbach, I. Barnes, K.H. Becker, E. Wiesen, Atmospheric chemistry of unsaturated carbonyls: Butenedial, 4-oxo-2-pentenal, 3-hexene-2,5-dione, maleic anhydride, 3*H*-furan-2one, and 5-methyl-3*H*-furan-2-one, Environ. Sci. Technol., 28 (1994) 715-729.

[9] B.G. Klotz, A. Bierbach, I. Barnes, K.H. Becker, Kinetic and mechanistric study of the atmospheric chemistry of muconaldehydes, Environ. Sci. Technol., 29 (1995) 2322-2332.

[10] R.A. Back, J.M. Parsons, The thermal and photochemical decomposition of maleic anhydride in the gas phase, Can. J. Chem., 59 (1981) 1342-1346.

[11] P. Veres, J.B. Gilman, J.M. Roberts, W.C. Kuster, C. Warneke, I.R. Burling, J. de Gouw, Development and validation of a portable gas phase standard generation and calibration system for volatile organic compounds, Atmos. Meas. Tech., 3 (2010) 683-691.

[12] C.E. Stockwell, A. Kupc, B. Witkowski, R.K. Talukdar, Y. Liu, V. Selimovic, K.J. Zarzana, K. Sekimoto, C. Warneke, R.A. Washenfelder, R.J. Yokelson, A.M. Middlebrook, J.M. Roberts, Characterization of a catalyst-based conversion technique to measure total particle nitrogen and organic carbon and comparison to a particle mass measurement instrument, Atmos. Meas. Tech., 11 (2018) 2749-2768.

[13] J.B. Burkholder, S.P. Sander, J. Abbatt, J.R. Barker, R.E. Huie, C.E. Kolb, M.J. Kurylo, V.L. Orkin, D.M. Wilmouth, P.H. Wine, "Chemical Kinetics and Photochemical Data for

Use in Atmospheric Studies, Evaluation No. 18," JPL Publication 15-10, Jet Propulsion Laboratory, Pasadena, 2015 http://jpldataeval.jpl.nasa.gov., (2015).
[14] C. Sousa, M. Agostinha, R. Matos, V.M.F. Morais, Experimental and computational thermochemical study of maleic anhydride and vinylene carbonate, J. Phys. Chem. A, 121 (2017) 9474-9484.
[15] Active Thermochemical Tables (ATcT), in, Argon National Laboratory, 2018.
[16] M.J. Frisch, G.W. Trucks, H.B. Schlegel, G.E. Scuseria, M.A. Robb, J.R. Cheeseman, G. Scalmani, V. Barone, G.A. Petersson, H. Nakatsuji, X. Li, M. Caricato, A.V. Marenich, J. Bloino, B.G. Janesko, R. Gomperts, B. Mennucci, H.P. Hratchian, J.V. Ortiz, A.F. Izmaylov, J.L. Sonnenberg, D. Williams-Young, F. Ding, F. Lipparini, F. Egidi, J. Goings, B. Peng, A. Petrone, T. Henderson, D. Ranasinghe, V.G. Zakrzewski, J. Gao, N. Rega, G. Zheng, W. Liang, M. Hada, M. Ehara, K. Toyota, R. Fukuda, J. Hasegawa, M. Ishida, T. Nakajima, Y. Honda, O. Kitao, H. Nakai, T. Vreven, K. Throssell, J.A. Montgomery Jr., J.E. Peralta, F. Ogliaro, M.J. Bearpark, J.J. Heyd, E.N. Brothers, K.N. Kudin, V.N. Staroverov, T.A. Keith, R. Kobayashi, J. Normand, K. Raghavachari, A.P. Rendell, J.C. Burant, S.S. Iyengar, J. Tomasi, M. Cossi, J.M. Millam, M. Klene, C. Adamo, R. Cammi, J.W. Ochterski, R.L. Martin, K. Morokuma, O. Farkas, J.B. Foresman, D.J. Fox, Gaussian 16, Revision A.03, Gaussian, Inc., Wallingford CT, 2016., in, 2016.

Maleic Anhydride

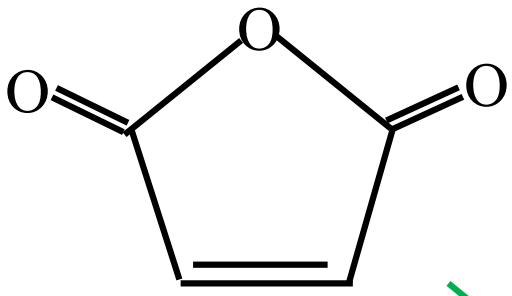

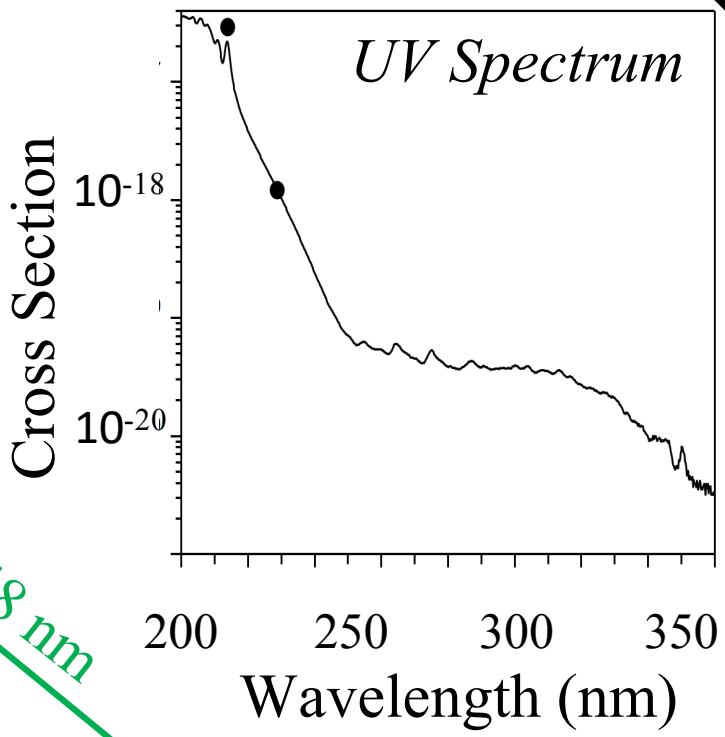

248 nm

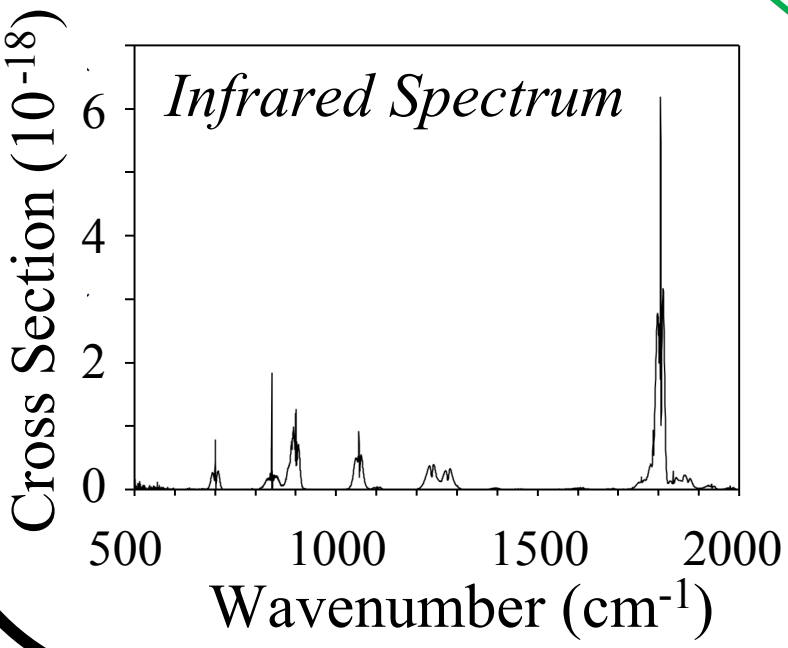

Quantum Yields

$\Phi(CO, CO_2, C_2H_2)$